

## Computation of a possible Tunguska's strewn field

ALBINO CARBOGNANI,<sup>1</sup> MARIO DI MARTINO,<sup>2</sup> AND GIOVANNA STIRPE<sup>1</sup>

<sup>1</sup>*INAF - Osservatorio di Astrofisica e Scienza dello Spazio  
 Via Gobetti 93/3  
 40129 Bologna, Italy*

<sup>2</sup>*INAF-Osservatorio Astrofisico di Torino  
 Via Osservatorio 20  
 10025 Pino Torinese (TO), Italy*

### ABSTRACT

On June 30, 1908 at about 0h 14.5m UTC what is known today as the Tunguska Event (TE) occurred, most likely caused by the fall of a small rocky asteroid of about 50-60 meters in diameter over the basin of the Tunguska River (Central Siberia). Unfortunately the first expedition was made by Kulik 19 years after the event and macroscopic meteorites have never been found in epicenter site. After considering the Chelyabinsk event as a guide, we estimated the strewn field of possible macroscopic fragments of the asteroid responsible of the TE: we have reason to believe that there might be fragments with enough strength to survive the airburst and reach the ground. The strewn field, which is located about 15 to 20 km North-West from the epicenter, forms an ellipse with axes from  $25 \times 20$  to  $40 \times 30$  km at  $3\sigma$  level and should be considered for the search of macroscopic bodies, even if the mud and vegetation could have made any trace disappear. Cheko Lake, which by some authors is considered an impact crater, falls about 3 km ( $\sim 4\sigma$ ) outside these areas and, based on our results, it is unlikely that it could be a real impact crater: only if the cosmic body's trajectory had an azimuth of about  $160^\circ - 170^\circ$  would be in the strewn field area, but it is not consistent with the most likely trajectory.

*Keywords:* minor planets — asteroids — Tunguska

### 1. INTRODUCTION

We define Tunguska-class asteroids as the near-Earth asteroids (NEAs) with a diameter between 10 and 100 meters, bodies that generally explode in the atmosphere before reaching the ground, unless their internal strength is particularly high. In a impact event with our planet, these bodies are not large enough to cause a global climate catastrophe but, thanks to the high fall speed and consequent great kinetic energy dissipation with strong shock waves, they are able to generate local airburst that, for larger objects in this class, it can be similar or worse than the Tunguska Event (TE) in Central Siberia.

In this area, on Jun 30, 1908 at 07:14:28 local time (00:14:28 UT), a small cosmic body of 50-60 meters in diameter exploded into the atmosphere about 8.5 km above the ground. In the explosion an energy around 15 Mt was developed which, in the form of a thermal wave and shock wave, destroyed an area of  $2150 \pm 50 \text{ km}^2$  of Siberian taiga. The first on-site scientific expedition was conducted in 1927 only - 19 years after the event - and is due to the Russian geologist Leonid Kulik. Despite the careful research conducted over the years by several expeditions around the catastrophe

epicenter, no macroscopic meteorite has ever been found despite the fierce excavation research conducted by Kulik in the epicenter area. For more details see [Longo \(2007\)](#), [Artemieva and Shuvalov \(2016\)](#) and references therein.

Most recent was the Chelyabinsk Event (CE) of Feb 15, 2013. At 03:20:20.8 UT a small asteroid with an estimated diameter of about  $20 \pm 5$  m begins the entry in the atmosphere toward the Russian city of Chelyabinsk (Lat.  $55^\circ 03'$  N, Long.  $61^\circ 08'$  E), located just East of the Ural mountains. About 11 s after entering into the atmosphere, at about 29.7 km altitude and 40 km South of Chelyabinsk, the pressure of the atmospheric shock wave becomes very strong and the asteroid explodes (main airburst), fragmenting into several pieces ([Popova et al. 2013](#)). We have several instrumental data about the CE, e.g. video recordings from surveillance cameras, satellite images and infrasonic data. This is a big difference respect the TE: as we will see better later there are visual testimonials, seismic and barometric registrations only.

Despite the small size of the asteroid causing the CE, a big meteorite weighing about 570 kg was found and collected on the bottom of the Lake Chebarkul, about 70 km West from

the airburst epicenter. A similar event may have happened for the TE also. In this hypothesis the epicenter area would not be the most suitable place to go in search for big meteorites. In other words, the devastation area of the Siberian Taiga is not necessarily the right place to look for macroscopic objects. Using the CE as a guide, we will delimit the area on the ground - i.e. the strewn field - to search for possible macroscopic meteorites belonging to TCB. About dark flight and strewn field computation, we have used the same procedure applied to the Italian fireball IT20170530 (Carbognani et al. 2020), to which we will refer as Paper I, which led to the successfully recovery of the Cavezzo meteorite on Jan 2020 (Gardiol et al. 2021).

That there are macroscopic fragments of the TCB is not obvious, also because until now they have never been found: the so called John's Stone, a meter-size quartzitic boulder near epicenter, most likely it is of terrestrial origin (Bonatti et al. 2015). For this reason the hypothesis that TCB was a comet has several supporters, however the statistics about the possible heliocentric orbits favor the asteroid hypothesis Farinella et al. (2001). Strictly speaking, the absence of macroscopic meteorites is not a proof of the complete disintegration of the TCB: the time elapsed from the fall to the first Kulik expedition was 19 years, enough time for any little craters and meteorites to be buried by mud and vegetation. In the scientific literature a reference regarding the existence of possible macroscopic fragments from the TE is in Artemieva and Shuvalov (2007), which mentions this possibility for cm-m sized fragments after simulating the TE using a hydrodynamic model with a strengthless falling body. The possible existence of macroscopic fragments with dimensions greater than 10 cm for the TE is reiterated in a 2016 paper of the same authors (Artemieva and Shuvalov 2016). This guess appear reasonable: the hydrodynamic model used is able to reproduce the shape and width of the devastation area caused by the shock wave, but cannot reproduce minor effects such as the survival and fall of macroscopic fragments. Other authors point out that the dynamic strength of decimetric rock objects entering the atmosphere is of the order of 1 MPa, therefore the arrival of large rocks on the ground in an energetic event such as that of Tunguska is very unlikely because they would completely disintegrate during the airburst (Collins et al. 2008). The issue is controversial, we will discuss it again in section 3.

## 2. THE CHELYABINSK EVENT

As a first step, we will use the data about the CE to test the dark flight and strewn field computation tools used in Paper I. Our aim is to predict the impact place of the largest fragment that survived the airburst. The main data available about the CE are listed in Table 1. Various individual fragmenta-

tions have been recorded between 40 and 30 km of altitude (Borovička et al. 2013). After the main airburst around 29.7 km, about 20 fragments emerged from the disruption clouds. The main boulder was destroyed at an altitude of 22 km, while another fragment - F1 in the Borovička's nomenclature - survived the fall in the densest layers of the atmosphere, survived a maximal dynamic pressure of about 15 MPa at an altitude of about 20 km, and began the dark flight phase at about 12.6 km height with a speed of 3.2 km/s over a point with latitude 54.9361° N and longitude 60.5883° E. The atmospheric path ended on the frozen surface of the Lake Chebarkul - with a ice layer thickness of about 70 cm - opening a hole of about 6 m in diameter. The azimuth of the trajectory of this fragment is practically identical to that of the progenitor body, with a deviation of about 1.3 degrees. So, after the main explosion, the progenitor of this big meteorite continued its motion practically along the main body's original trajectory.

### 2.1. Fragments separation

The fact that, after meteoroid fragmentation, the major fragments continue to follow about the same trajectory as the original body is well known. There are several effects which cause dispersion of the meteoroid fragments, as gravity, atmospheric drag, lift or bow shock interaction just after fragmentation. Drag and gravity forces are dominant for trajectory inclination angle less than about 30°, while for higher inclinations the separation is due to the bow shock interaction (Passey and Melosh 1980).

Not only larger fragments receive lower lateral acceleration, but if they are larger than about 1/16 of the main body (for the CE this means bodies with at most ~ 1 meter in diameter while for the TE bodies with at most ~ 4 meters in diameter), the primary shock wave prevents them from escaping. On the other hand, smaller bodies can be expelled out of the shocked region by aerodynamic effects (Laurence et al 2007). In both cases small fragments have significantly different trajectories respect to larger fragments.

This is exactly what happened in the case of CE. With an inclination of the trajectory well below 30° gravity and atmospheric drag forces dominated in the separation of the fragments. Meteorites of about 0.1 g fall near the point of main explosion, masses of about 100 g fell further along the trajectory, and at least one of 3.4 kg fall near Timiryazevskiy (Popova et al. 2013). All these minor fragments were subject to an acceleration along the trajectory given by (Passey and Melosh 1980):

$$\frac{dV}{dt} \propto -\frac{V^2}{M/A} + g \sin(\theta) \quad (1)$$

In Eq. (1)  $V$  is the body's speed respect to air,  $M$  is the mass,  $A$  the fragment's cross section,  $g$  the gravity acceleration and

$\theta$  the trajectory inclination respect to ground. Considering that the mass-area ratio  $M/A$  is proportional to the fragment's radius, smaller the meteoroid and greater the negative acceleration will be. This caused smaller fragments to fall much earlier than the fragment F1.

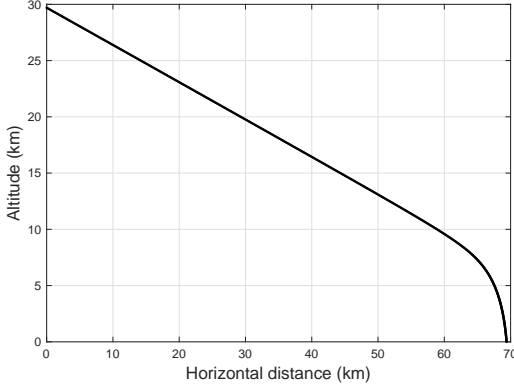


**Figure 1.** The nominal dark flight trajectory for the Chelyabinsk biggest fragment with  $M/A \approx 1600$ . The starting point is from the main explosion and the nominal impact point is about 69.4 km away from the epicenter, very close to the real one.

## 2.2. Dark flight of the F1 fragment

The fragment F1 from the CE was recovered in the Lake Chebarkul on Oct 16th and found to weigh about 570 kg. Considering that the bulk density of the Chelyabinsk meteorites is  $3290 \text{ kg/m}^3$  (Kohout et al. 2013), an effective size of about 0.7 m and a mass-area ratio of about  $1500 \text{ kg/m}^2$  can be estimated. Taking into account the residual fragmentation during impact, the impacting mass may have been 600–650 kg (Popova et al. 2013), for an original mass-area ratio of about  $1600 \text{ kg/m}^2$ .

To put us in a condition similar to that of Tunguska, i.e. with very little data, we will describe the three-dimensional motion of the main fragment F1 using essentially Newton's Resistance law from Eq. (1), see Paper I and Cephecha (1987) for more details. As altitude, inclination, azimuth and starting speed for the dark flight computation we use the data reported in Table 1 for F1. In order to model the dark flight phase, it is important to know the atmospheric profile in the data, time and place closest to the fall because the residual meteoroid trajectory can be heavily influenced by the atmospheric conditions, especially in the case of strong winds in the lower layers of the atmosphere. The influence of weather conditions diminishes as the size and speed of the fragment increases.

The wind profile for the CE was taken from atmospheric sounding conducted by the Verkhneye Dubrovo station ( $56.73^\circ \text{ N}$ ,  $61.06^\circ \text{ E}$ ) - the weather station nearest to Chelyabinsk - at 0:00 UT. The computed impact coordinates for F1 are long.  $60.30^\circ \text{ N}$  and lat.  $54.96^\circ \text{ E}$ . These impact

**Table 1.** Data about atmospheric trajectory of the Chelyabinsk event and the hole in the Chebarkul lake (Popova et al. 2013). The data about the major fragment F1 refer to the beginning of the dark flight phase (Borovička et al. 2013). Azimuth is clockwise from North.

Quantity	Best Value
$H_{\text{start}}$ (km)	$97.1 \pm 2$
$v_\infty$ (km/s)	$19.2 \pm 0.3$
Entry elevation angle ( $^\circ$ )	$18.3 \pm 0.2$
Entry azimuth ( $^\circ$ )	$103.2 \pm 0.4$
Entry latitude ( $^\circ$ )	$54.44 \pm 0.02 \text{ N}$
Entry longitude ( $^\circ$ )	$64.56 \pm 0.03 \text{ E}$
Main peak altitude (km)	$29.7 \pm 0.7$
Main peak latitude ( $^\circ$ )	$54.84 \pm 0.02 \text{ N}$
Main peak longitude ( $^\circ$ )	$61.41 \pm 0.03 \text{ E}$
Main peak speed (km/s)	$19.2 \pm 0.2$
F1 height (km)	12.57
F1 speed (km/s)	3.2
F1 latitude ( $^\circ$ )	54.9361
F1 longitude ( $^\circ$ )	60.5883
F1 azimuth ( $^\circ$ )	$101.87 \pm 0.4$
F1 elevation angle ( $^\circ$ )	$17.53 \pm 0.3$
Hole Chebarkul Lake latitude ( $^\circ$ )	$54.95976 \pm 0.00006 \text{ N}$
Hole Chebarkul Lake longitude ( $^\circ$ )	$60.32087 \pm 0.00006 \text{ E}$
Hole diameter (m)	$6.3 \pm 0.5$

coordinates are about 19 km away from the starting point, with a difference of about 1.4 km respect to the real observed impact point. Considering the path length of the dark flight and the simplifications adopted this appear a good result.

The result does not change significantly even assuming the epicenter of the main explosion (height 29.7 km) as the starting point for the dark flight, with a speed identical to that of the main body entering the atmosphere, i.e. 19.2 km/s. Neglecting the still active ablation process and the effects of the shock wave as impact point we found long.  $60.35^\circ \text{ N}$  and lat.  $54.98^\circ \text{ E}$ . These impact coordinates are about 69.4 km away from the main epicenter, with a difference of about 3 km respect to the real impact point (see Fig. 1). Given the low sensitivity of the impact point position respect to the starting dark flight condition we apply the same technique to estimate the position and extent of the Tunguska strewn field for macroscopic meteorites.

## 2.3. Effective strength of the Chelyabinsk event

Before moving to the TE we will calibrate a strength relationship using the data available about Chelyabinsk. Usually the meteoroids fragmentation model assume that the process starts when the aerodynamic pressure  $P_{\text{dyn}} = \Gamma \rho_{\text{fr}} V^2$  in front of the body which moves with speed  $V$ , is equal or super-

prior to mechanical strength  $S$ :  $P_{dyn} \geq S$  (Passey and Melosh 1980; Svetsov et al. 1995; Farinella et al. 2001). The quantity  $\rho_{fr}$  is the atmospheric density at fragmentation level,  $V$  is the body's speed respect to air while  $\Gamma$  is the dimensionless drag coefficient (for a spherical body  $\Gamma = 0.5$ ). However, the hypersonic air flow around the body is turbulent and the turbulent shock wave locally increases the dynamic pressure exerted on meteoroid. Accordingly, large meteoroids can fragment at lower dynamic pressures than their mechanical strength and the condition for fragmentation (not for airburst) can be written as follows (Foschini 2001):

$$S = \bar{k}\Gamma(1 + \alpha)\rho_{fr}V^2 \quad (2)$$

In Eq. (2)  $\bar{k}$  is the pressure amplification factor due to the interaction between turbulence and shock wave while the number  $\alpha \approx 1$  is the coefficient of ionization for the plasma state. We can estimate the value of the air fragmentation density,  $\rho_{fr}$ , using a isothermal atmospheric model with a mean scale height  $H_0 \approx 7.64$  and density at sea level  $\rho_0 \approx 1.29 \text{ kg/m}^3$ , so (Foschini 2001):

$$\rho_{fr} \approx \rho_0 e^{-(h+H_0)/H_0} \quad (3)$$

In Eq. (3)  $h$  is the height of the observed airburst, while  $h+H_0$  is an estimate of the fragmentation's height: the fragmentation is not an instantaneous process and start at a higher altitude than airburst, as confirmed from collected data. The problem with Eq. (2) is that the  $\bar{k}\Gamma(1 + \alpha)$  factor is not known a priori, mainly for the  $\bar{k}$  value. In the case of Chelyabinsk we can estimate it using the strength measured on the recovered meteorites. However, the strength of the meteorites does not coincide with the original body's strength.

For example, in the case of the major fireballs observed by the European Fireball Network the original meteoroid has a dynamic strength always lower respect the subsequent fragmentations: the strength of first fragmentation is in the range 0.4-4 MPa while the main fragmentation is in the range 3.5-12 MPa (Borovička et al. 2008). This difference is probably due to fractures present in large meteoroids or small asteroids which decrease the overall strength of the original body compared to the individual non-fractured blocks (Popova et al. 2011). Put simply, the strength of the original body is the lower limit of the strength of the blocks into which it can separate as it crosses the atmosphere.

If the mechanical destruction of a body occurs along the fracture lines, then it is reasonable to expect that the strength depends on the volume or mass and that the following scale relation holds (Weibull 1951; Svetsov et al. 1995):

$$S_{main} = S_{fr} \left( \frac{m_{fr}}{m_{main}} \right)^\alpha \quad (4)$$

In Eq. (4), based on Weibull's statistical strength theory,  $\alpha$  is the scale factor,  $S_{main}$  is the main body strength while  $S_{fr}$

is the fragment strength. The same hold for the masses  $m$ . The  $\alpha$  value increases as the inhomogeneity of the material increases and a value between 0.1 and 0.5 is expected. In the case of Chelyabinsk, the  $\alpha$  value can be directly estimated from the mechanical strength and mass values measured on meteorites. Mechanical properties of the Chelyabinsk meteorite were determined at NASA Ames and compression strength is determined to be 330 MPa (C3: 4.46 g), 327 MPa (C4: 4.84 g) and 408 MPa (C5: 1.58 g), similar to other ordinary chondrites (Popova et al. 2013). Using Eq. (4) and these meteorites data we get  $\alpha \approx 0.2$ , a reasonable value within the expected range. From the total mass estimated for Chelyabinsk, about  $1.4 \cdot 10^7 \text{ kg}$  and from the average strength of the two major samples, we find  $S_{CE} \approx 4 \text{ MPa}$  as in Foschini et al. (2019). This value is in good agreement with Borovička et al. (2013) which finds  $S \approx 1 \text{ MPa}$ , it is only greater than a factor 4. About the same  $\alpha$  value is found using the Borovička's strengths for the main mass and the F1 fragment ( $\sim 15 \text{ MPa}$ ).

With this estimate of the effective mechanical strength of Chelyabinsk we can evaluate the factor  $\bar{k}\Gamma(1 + \alpha)$  in Eq. (2). From Eq. (3) with  $h = 29.7 \text{ km}$ , we have  $\rho_{fr} \approx 0.01 \text{ kg/m}^3$ , so reversing Eq. (2) with  $V = 19.2 \text{ km/s}$  and  $S \approx 4 \text{ MPa}$  we get  $\bar{k}\Gamma(1 + \alpha) \approx 1.1$ . Considering that for a plasma state, as expected for little asteroids fall,  $\alpha \approx 1$  and that  $\Gamma \approx 0.5$ , it follow that  $\bar{k} \approx 1.1$ , a value greater than 1, as expected.

### 3. THE TUNGUSKA EVENT

While for the CE the available data are abundant, for the TE instrumental values are scarce, the most reasonable data are reported in Table 3. The uncertainties in this table - apart the speed values - are the standard deviation of the mean values given by various authors and summarized in the table 18.1 of the Longo (2007) work. Our paper is not intended to re-discuss the results about Tunguska, so we limit ourselves to some essential points.

About the TE there are seismic and barometric registration recorded immediately after the event and data on forest devastation about directions of flattened trees and charred trees, collected in a century of on field expeditions. The time of the event was established reasonably well from the seismic and barometric recordings. The most widely quoted magnitude range of the developed energy, based on historic barograms, seismic records, and forest damage is between 10 and 40 Mt with a more probable value of about 15 Mt (Vasilyev 1998), even though Boslough and Crawford (1997, 2008), on the basis of the results of numerical simulations, estimated an energy of 3-5 Mt.

Finally, from forest devastation, an explosion height of about 8.5 km was obtained (Ben-Menahem 1975). The geographic coordinates on the ground of the explosion in the atmosphere (the so called epicenter) was set by the azimuth distribu-

tion of the flattened trees, while from the symmetry of the devastation area and eyewitness data the range for trajectory azimuth and inclination above Earth surface was set (Farinella et al. 2001; Longo 2007).

### 3.1. The speed and strength problems

The most critical parameter to set, very important both to obtain the heliocentric orbit and the dark flight phase of hypothetical macroscopic fragments, is the TCB's atmospheric speed. Being a body of 50-60 meters in diameter, the speed loss due to atmospheric friction can be considered negligible as in the CE case and the geocentric speed - if the TCB belong to solar system - can range from about 11.2 to 70 km/s (Passey and Melosh 1980). As we see better in section 3.2, considering the range of the possible atmospheric trajectories, the geocentric speed cannot be greater than about 35 km/s because the body could not belong to the solar system. As a starting hypothesis in order to estimate the TCB's mechanical strength we can assume that  $\bar{k}\Gamma(1+\alpha)$  is equal to that of Chelyabinsk. From Eq. (2), with  $h \approx 8.5$  km,  $\rho_{fr} \approx 0.16$  kg/m<sup>3</sup> and  $V$  in the range 11-35 km/s we find  $S \approx 20 - 200$  MPa, see Fig. 2. So we can say that, despite the falling velocity into the atmosphere remains the most difficult parameter to estimate, the mechanical strength of TCB was superior to that of Chelyabinsk.

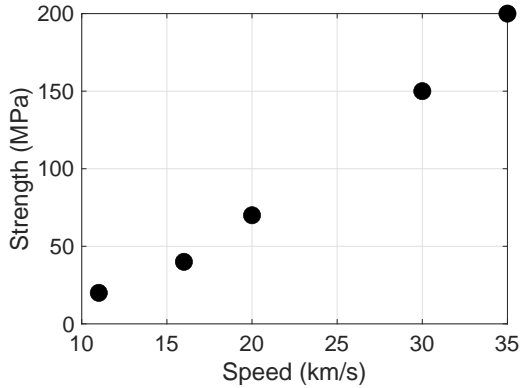


**Figure 2.** The TCB's strength as a function of the possible speed in the atmosphere computed for an airburst altitude of 8.5 km.

Considering the mechanical strength values measured in laboratory on rocky meteorites, from 6 to 200 MPa for compressive strength and from 2 to 62 MPa for tensile strength (Svetsov et al. 1995), physically reasonable values for TCB's strength range from 20 to 100 MPa, corresponding to an atmospheric speed between 11 and 20 km/s, typical values for an asteroidal origin. Based on these raw estimates, the effective strength of Tunguska's body appears at least 5 times higher than CE. That TCB was considerably stronger than Chelyabinsk also follows from the need of different

**Table 2.** The percentage of asteroid or cometary closed heliocentric orbits as a function of the TCB's speed. Of the 4000 possible simulated orbits, 3373 are closed and about 70% of these are asteroidal-type, while the remaining 30% are cometary-type.

$V$ (km/s)	Asteroids (%)	Comets (%)	Closed orbits (%)
$16 \pm 5$	97	3	100
$20 \pm 5$	91	9	99.0
$30 \pm 5$	47	53	82.5
$35 \pm 5$	18	82	55.8

airbursts models (pancake, debris cloud and chain reaction) to converge at the same estimated explosion height for the TE (Morrison 2018). The fact that the strength of TCB was at least 20 MPa and the empirical rule that the original body has a tensile strength always lower than fragments (Scheeres et al. 2015), see Eq. (4), leads us to hypothesize that TCB was composed of compact rock blocks. From Eq. (4) with  $\alpha \approx 0.2$ ,  $m_{main} \approx 4 \cdot 10^8$  kg and  $S_{main} \geq 20$  MPa, we found  $S_{fr} \geq 200$  MPa for a fragment with a diameter of about 1 m, and  $S_{fr} \geq 100$  MPa for a fragment of about 4 m, i.e. the macroscopic fragments small enough to escape the shock wave appear potentially able to resist the airburst phase. These fragments appear large enough to survive the intense ablation phase during the airburst while the smaller fragments, 3-10 cm in diameter, vaporize (Svetsov 1996).

Obviously we do not know the real structure of the TCB: it was monolithic, rubble pile or somewhere between these two possible structures? The existence of monolithic blocks with dimensions up to several tens of meters is confirmed by the space exploration of asteroids with rubble pile structure, such as Ryugu (Michikami et al 2019) and Bennu (Jawin et al. 2019). Furthermore, the measurements of thermal inertia conducted by the OSIRS-REX mission on the Bennu boulders have shown that there are two rock types: low and high tensile strength, with a factor about 8 between the two categories (from 0.1 MPa to 0.8 MPa), see Rozitis et al. (2020). This shows how variable the strength of a monolithic boulder on asteroid surface can be. The fall of Carancas, which took place in Peru on September 15, 2007, is emblematic: in this case there was no fragmentation and the rocky meteoroid arrived intact on the ground, generating a crater 13 m in diameter near Lake Titicaca. The estimated starting speed for this monolithic body, with dimension in the range 0.9-1.7 m, is under 23 km/s and the dynamic strength ranges from 20 to 40 MPa, values much higher than 0.4-12 MPa valid for small meteoroids. So in our picture, TCB was a little rocky asteroid with high tensile strength which allowed an airburst within the troposphere, but composed of pieces of rock even stronger probably able to survive the explosion and reach the ground.

**Table 3.** Data about the the TE (Longo 2007). The RA and DEC of the apparent radiant have been computed starting from azimuth and elevation. The epicenter coordinates is from the basis of fallen trees (Fast 1967; Longo et al. 2005).

Quantity	Best Value
Entry elevation angle (°)	$15 \pm 5$
Entry azimuth <sup>a</sup> (°)	$110 \pm 10$
RA apparent radiant (°)	$89 \pm 10$
DEC apparent radiant (°)	$4 \pm 6$
Time of explosion (UT)	0h 14m 28s
Height of explosion (km)	$8.5 \pm 2$
Energy of explosion (Mt)	$\sim 15$
Epicenter Latitude (°)	$60.886 \pm 0.02$ N
Epicenter Longitude (°)	$101.894 \pm 0.02$ E
Speed range (km/s)	$15 - 21 (18 \pm 3)$

<sup>a</sup> Clockwise from North

### 3.2. TCB's orbit

Taking into account the possible parameters of the ground trajectory (azimuth, inclination, altitude of the explosion) given in Table 3, we explored different speed ranges:  $16 \pm 5$ ,  $20 \pm 5$ ,  $30 \pm 5$  and  $35 \pm 5$  km/s to compute the possible heliocentric orbits. For higher speeds the TCB no longer belongs to the solar system, because the heliocentric speed is higher than escape velocity from the Sun at the Earth's distance. For each velocity interval, 1000 clones compatible with the parameters of the observed ground trajectory were used and correcting for Earth's rotation and gravity attraction (Ceplecha 1987), the corresponding heliocentric orbits have been obtained. Considering only closed orbits they were classified using the Tisserand parameter with respect to Jupiter ( $T_J$ ) because, in first approximation, it is able to discriminate between asteroidal orbit ( $T_J \geq 3$ ) and cometary orbit ( $T_J < 3$ ). The result tell us that about 70% of the orbits are of asteroidal origin, while the remaining 30% are of cometary origin. This result is in good agreement with Farinella et al. (2001) that exploring the ranges 14-16 km/s, 30-32 km/s and considering  $T_J$  as a parameter for orbit classification had found 77% of asteroidal orbits and 23% of cometary orbits. From a statistical point of view, the asteroidal origin for the TCB continues to remain the most favored one, see Table 2.

### 3.3. Tunguska's dark flight and strewn field

As in the case of Chelyabinsk, to compute the trajectory followed by the possible macroscopic fragments that survived the explosion of the main body, is necessary to know the height, azimuth, inclination of the trajectory and the starting speed. These values, with their uncertainties, are taken from Table 3.

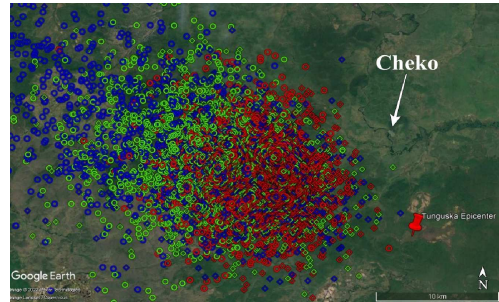


**Figure 3.** The strewn fields for the TE computed for fragments with  $M/A$  as in Table 4. Circles are for low inclination trajectory, squares for hight inclination. In red the lightest meteorites, in blue the most massive ones. Cheko Lake is indicated by the white arrow and is about 3 km from the Eastern edge of the combined strewn fields.

As atmospheric profile we chose the NRLMSISE-00 model (Picone et al. 2002), computed for the coordinates and the date of the atmospheric explosion. Considering that our aim is to trace the largest fragments shown in Table 4, the exact winds profile is not very important, and this is a fortunate circumstance because there are no atmospheric profiles of wind speed and direction for the TE. To compute the uncertainty of the strewn field we used a Monte Carlo approach, as for the origin of the orbits, generating 1000 different scenarios for each fragment and looking at the geographic distribution of the possible fall zones. In Fig. 4 and Fig. 5 two possible trajectories are shown for the dark flight phase of two fragments at the limits of the size range adopted.

Unlike the CE there are important differences from the low inclination of the trajectory estimated by the eyewitnesses and that obtained from the analysis of the devastation area. In this last case the best estimate are for angles of about  $30^\circ$ , the double of the  $15^\circ$  adopted in Table 3 (Vasilyev 1998; Longo et al. 2005). So, for completeness, we have computed the strewn field even for an inclination of  $30 \pm 5$  degrees. Due to the higher inclination, the strewn field is closer to the epicenter and less dispersed than in the previous case.

The result of our computation, in the case of low inclination, is that the strewn field for the TE is about 20 km WNW away from the epicenter, see Table 4. Due to the great uncertainties involved the strewn field is quite large: at  $3\sigma$  level it forms an ellipse with mean center at long.  $101.44^\circ$  N, lat.  $60.96^\circ$  E and axes about  $40 \times 30$  km, for an area of about  $\pi \cdot 20 \cdot 15 \approx 1000$  km $^2$ . In the case of higher inclination the distance from the epicenter is about 15 km WNW with axes  $25 \times 20$  km, but there are no substantial qualitative changes compared to the first case, see Fig. 3.

### 3.4. About the Lake Cheko origin

**Table 4.** Size  $D$  of the hypothetical macroscopic fragments of the TE as a function of the  $M/A$  ( $\text{kg/m}^2$ ) ratio assuming an average density of  $\rho \approx 3500 \text{ kg/m}^3$ , typical of chondrites. The nominal coordinates of the center of the strewn field are also shown (the suffixes of Lat. and Long. stand for  $L \approx 15^\circ$  and  $H \approx 30^\circ$  inclination trajectory): the coordinates difference decreases as the size of the test meteoroid increases because the atmosphere has less and less influence.

$M/A$	$D$ (m)	Lat.L ( $^\circ$ )	Long.L ( $^\circ$ )	Lat.H ( $^\circ$ )	Long.H ( $^\circ$ )
10,000	4.3	60.99	101.32	60.93	101.64
5000	2.0	60.98	101.38	60.93	101.64
3000	1.3	60.96	101.44	60.93	101.64
1600	0.7	60.94	101.55	60.92	101.66
1000	0.4	60.93	101.67	60.92	101.70

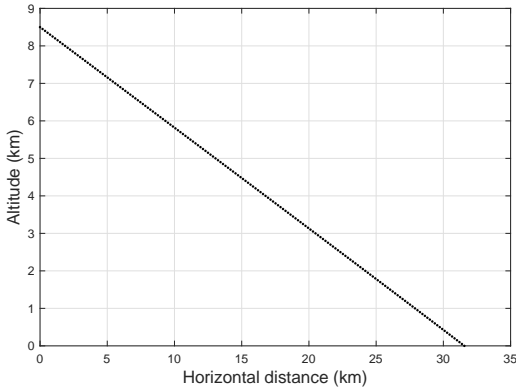


**Figure 4.** The nominal dark flight trajectory for  $M/A \approx 10,000 \text{ kg/m}^2$ , inclination about  $15^\circ$  and  $V = 18 \text{ km/s}$  shows that the atmospheric influence is negligible with the nominal impact point about 32 km away from the epicenter.

These results about a possible strewn field give us the opportunity to make some comments about the Cheko lake, a small lake elliptical in shape with axes equal to  $500 \times 350$  m elongated in NW-SE direction, located about 9 km in a direction with azimuth of  $348^\circ$  from the epicenter. Cheko lake is considered by some authors as a possible impact crater (Gasperini et al. 2007, 2008, 2009, 2014). The most intriguing clues about this lake are the conical shape, the density/velocity discontinuity in the center of the lake about 10 m below the bottom (the so called reflector-T) and the trees near the shores of the lake that show vigorous growth only after 1908 until present day, suggesting that they are born when there was no lake (Gasperini et al. 2014; Fantucci et al. 2015). The scientific debate about lake Cheko's origin is still open and several authors do not consider it as an impact structure: there is no sure evidence that the lake is only 100 years old and it is strange that a single impact structure formed during the TE because crater fields are usually found, furthermore the edge of the lake is not as prominent as one

would expect from an impact crater (Collins et al. 2008).

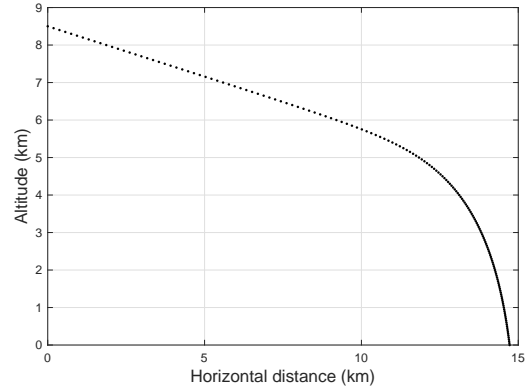


**Figure 5.** The same of Fig. 4 but with  $M/A \approx 1000 \text{ kg/m}^2$ . In this case the atmosphere deflects the trajectory in the final part and the nominal impact point is about 15 km from the epicenter.

On the basis of our findings, Cheko lake is outside from the more likely strewn field because is about 3 km from the external boundary that defines the zone, i.e. about  $4\sigma$  from the strewn field center. Making computations of the strewn field by varying the trajectory's azimuth we find that the lake could be an impact crater if the azimuth of the trajectory traveled by the TCB were between  $160$  and  $170$  degrees. These values are in agreement with the fact that to joining the epicenter with the lake the incoming trajectory would have an azimuth of  $348^\circ - 180^\circ \approx 168^\circ$ . However, these values are distant from the most common azimuth value adopted here ( $110^\circ \pm 10^\circ$ ). The value for the azimuth of the trajectory closest to  $168^\circ$  is that of  $137^\circ$  obtained by Krinov (1949), based on eyewitness accounts of the fireball. On the other hand, is unlikely that the value of  $110^\circ \pm 10^\circ$  be far from reality. The area of the trees fall resembles a triangle or a butterfly and has an axis of symmetry directed towards an azimuth of about  $115^\circ$  (Artemieva and Shuvalov 2016): with this condition it is difficult to think that the trajectory of the TCB could have been directed towards the lake. A deviation of at least  $50^\circ$  would be necessary, but this is almost impossible for a macroscopic fragment generated in the epicenter. Our result is in agreement with Foschini et al. (2019), which make the hypothesis that the TCB may have been a binary asteroid to justify the formation of the Cheko Lake as an impact crater. This complex scenario is necessary because the lateral speed of the big meteoroid necessary to create the lake is too small to obtain a significant deviation from the original trajectory, so it is not possible for a large fragment to form an impact crater in the Cheko zone. This would be theoretically possible in the case of a binary asteroid, with a small object in orbit around the main body. The binary asteroid hypothe-

sis would also solve the problem of the absence of a craters field.

#### 4. CONCLUSIONS

Using the CE as a reference, we have verified that the simple equation for the atmospheric drag is sufficient to obtain, with a good approximation, the fall zone of the fragment F1 and we have also calibrated a relationship that allows to pass from the airburst height to the body's strength. In this way, assuming a reasonable range of atmospheric speeds, we estimated the TCB's strength finding it about 5 times higher than the Chelyabinsk asteroid. Using the strength's law scale this lead us to believe that the TCB could be composed of high strength boulders capable of reaching the ground after the airburst. Considering the uncertain parameters of the TCB's atmospheric trajectory, we have computed a possible strewn field for big meteorites in the theoretical range 0.4-4 m. The strewn field center for low trajectory inclination is located about 20 km WNW away from the TE epicenter with an extension of about  $40 \times 30$  km at  $3\sigma$  level. For hight trajectory inclination the strewn field is 15 km WNW with an extension

of about  $25 \times 20$  km. If some macroscopic meteorites were produced following the TE, this is the most likely regions to look for. Unfortunately, the time elapsed from the fall of the TCB to the first Kulik expedition was 19 years, enough time for any little craters and meteorites to be buried by mud and vegetation. This is even more true today because more than a century has passed while Siberian taigá is still very inhospitable and difficult to explore. Lake Cheko is about 3 km outside this large area and, based on our results, it is unlikely that it could be a real impact crater unless the trajectory of the TCB had an azimuth between  $160^\circ$  and  $170^\circ$ . However, this value is in contrast with the azimuth of the axis of symmetry of the area of the trees fall, about  $115^\circ$ . We also verified that, based on the most probable parameters for the atmospheric trajectory of the TCB, about 70% of the possible closed heliocentric orbits are compatible with an asteroidal origin.

#### DATA AVAILABILITY

The data underlying this article will be shared on reasonable request to the corresponding author.

#### REFERENCES

Artemieva, N., Shuvalov, V., 2007. 3D effects of Tunguska event on the ground and in the atmosphere. *Lunar Planet. Sci.*, XXXVIII (Abstracts), 1537.

Artemieva, N., Shuvalov, V., 2016. From Tunguska to Chelyabinsk via Jupiter. *Annual Review of Earth and Planetary Sciences*, 44, 37-56.

Ben-Menahem, A., 1975. Source parameters of the siberian explosion of June 30, 1908, from analysis and synthesis of seismic signals at four stations. *Phys. Earth Planet. Inter.* 11, 1-35.

Bonatti, E., et al., 2015. Origin of John's Stone: A quartzitic boulder from the site of the 1908 Tunguska (Siberia) explosion. *Icarus* 258, 297-308.

Borovička, J., Spurný, P., 2008. The Carancas meteorite impact - Encounter with a monolithic meteoroid. *Astronomy & Astrophysics*, 485, L1-L4.

Borovička, J., et al., 2013. The trajectory, structure and origin of the Chelyabinsk asteroidal impactor. *Nature*, 503, 235-237.

Boslough, M. and Crawford, D.A., 1997, In J.L. Remo, Ed., *Near-Earth Objects*, Annals of the New York Academy of Sciences, V822, 236-282.

Boslough, M. and Crawford, D.A., 2008. Low-altitude airbursts and the impact threat. *International Journal of Impact Engineering*, 35, 1441-1448.

Carbognani, A. et al., 2020. A case study of the May 30, 2017, Italian fireball. *Eur. Phys. J. Plus*, 135, 255.

Ceplecha, Z., 1987. Geometric, dynamic, orbital and photometric data on meteoroids from photographic fireball networks. *Bulletin Astronomical Institutes of Czechoslovakia*, 38, 222-234.

Collins, G. S. et al., 2008. Evidence that Lake Cheko is not an impact crater. *Terra Nova*, 20, 165-168.

Fantucci, R. et al., 2015. The Tunguska event and Cheko lake origin: dendrochronological analysis. *International Journal of Astrobiology*, 14, 345-357.

Farinella, P. et al., 2001. Probable asteroidal origin of the Tunguska Cosmic Body. *Astronomy & Astrophysics*, 377, 1081-1097.

Fast V. G., 1967, Statisticheskij analiz parametrov Tungusskogo vyvala, in *Problema Tungusskogo meteorita*, Izdatelstvo Tomskogo Universiteta, Tomsk, part 2, 40-61.

Foschini, L., et al., 2019. The atmospheric fragmentation of the 1908 Tunguska Cosmic Body: reconsidering the possibility of a ground impact. <https://arxiv.org/abs/1810.07427>.

Foschini, L., 2001. On the atmospheric fragmentation of small asteroids. *Astronomy & Astrophysics*, 365, 612-621.

Gardioli, D. et al., 2021. Cavezzo, the first Italian meteorite recovered by the PRISMA fireball network. *Orbit, trajectory, and strewn-field*. *MNRAS*, 501, 1215-1227.

Gasperini, L. et al., 2007. A possible impact crater for the 1908 Tunguska Event. *Terra Nova*, 19, 245-251.

Gasperini, L. et al., 2008. Lake Cheko and the Tunguska Event: impact or non-impact? *Terra Nova*, 20, 169-172.

Gasperini, L. et al., 2009. Sediments from Lake Cheko (Siberia), a possible impact crater for the 1908 Tunguska Event. *Terra Nova*, 21, 489-494.

Gasperini, L. et al., 2014. The origin of Lake Cheko and the 1908 Tunguska Event recorded by forest trees. *Terra Nova*, 26, 440-447.

Kohout, M. et al., 2013. Mineralogy, reflectance spectra, and physical properties of the Chelyabinsk LL5 chondrite. *Meteoritics and Planetary Science*, 48, A205.

Krinov, E. L., 1949, Tungusskij meteorit, Izdatelstvo Akademii Nauk SSSR, Moskva Leningrad.

Jawin, E. R., 2019, 50th Lunar Planet. Sci. Conf., (Abstracts), 2132.

Longo, G. et al., 2005, In: Asteroid comet Hazard-2005, (M. Smelror, H. Dypvik and F. Tsikalas, eds). Institute of Applied Astronomy of the Russian Academy of Sciences, St Petersburg, 222-225.

Longo, G., 2007. The Tunguska Event. In the book: *Comet/Asteroid Impacts and Human Society*, Springer-Verlag, Berlin Heidelberg New York.

Laurence, S. J., 2007. Proximal bodies in hypersonic flow. *Journal of Fluid Mechanics*, 590, 209-237.

Michikami, T. et al., 2019. Boulder size and shape distributions on asteroid Ryugu. *Icarus*, 331, 179-191.

Morrison, D., 2018. Tunguska Workshop: Applying Modern Tools to Understand the 1908 Tunguska Impact. NASA/Technical Memorandum - 220174.

Passey, Q. R., Melosh H. J., 1980. Effects of Atmospheric Breakup on Crater Field Formation. *Icarus*, 42, 211-233.

Picone, J. M., et al., 2002. NRLMSISE-00 empirical model of the atmosphere: Statistical comparisons and scientific issues. *Journal of Geophysical Research (Space Physics)*, 107, 1468.

Popova, O. P. et al., 2011. Very low strengths of interplanetary meteoroids and small asteroids. *Meteoritics & Planetary Science*, 46, Issue 10, 1525-1550.

Popova, O. P. et al., 2013. Chelyabinsk airburst, damage assessment, meteorite recovery, and characterization. *Science*, 342, Issue 6162, 1069-1073.

Rozitis, B. et al., 2020. Asteroid (101955) Bennu's weak boulders and thermally anomalous equator. *Science Advances*, 6, Issue 41.

Scheeres D. J., Britt D., Carry B., Holsapple K. A, 2015, Asteroid interiors and morphology. In *Asteroids IV*, 745-766.

Svetsov V. V. et al., 1995. Disintegration of Large Meteoroids in Earth's Atmosphere: Theoretical Models. *Icarus*, 116, 131-153.

Svetsov V. V., 1996. Total ablation of the debris from the 1908 Tunguska explosion. *Nature*, 383, 697-699.

Vasilyev N. V., 1998. The Tunguska Meteorite problem today. *Planet Space Sci.*, 46, 129-150.

Weibull, W., 1951. A Statistical Distribution Function of Wide Applicability. *Journal of Applied Mechanics*, 103, 293-297.